

# Active Vibration Control of Piezolaminated Smart Beams

V. Balamurugan

*Combat Vehicles Research & Development Establishment, Chennai – 600 054*

and

S. Narayanan

*Indian Institute of Technology Madras, Chennai – 600 036*

## ABSTRACT

This paper deals with the active vibration control of beam like structures with distributed piezoelectric sensor and actuator layers bonded on top and bottom surfaces of the beam. A finite element model based on Euler-Bernoulli beam theory has been developed. The contribution of the piezoelectric sensor and actuator layers on the mass and stiffness of the beam is considered. Three types of classical control strategies, namely direct proportional feedback, constant-gain negative velocity feedback and Lyapunov feedback and an optimal control strategy, linear quadratic regulator (LQR) scheme are applied to study their control effectiveness. Also, the control performance with different types of loading, such as impulse loading, step loading, harmonic and random loading is studied.

**Keywords:** Active vibration control, beam theory, smart beams, piezoelectric sensors, piezoelectric actuators, active vibration, beam theory, finite element model, feedback control

## 1. INTRODUCTION

The increasing demand of high structural performance requirements has led to the development of smart/intelligent materials and structures. A smart or intelligent structure involves distributed actuators and sensors, and one or more microprocessors that analyse the response from the sensors and use distributed parameter control theory to command the actuators to apply localised strains. A smart structure has the capability to respond to changing external environment (such as loads, temperature and shape) as well as to changing internal environment (such as damage or

failure). This technology has numerous applications, such as active vibration and buckling control, shape control, damage assessment and active noise control. The development of these smart or intelligent structures offer great potential for use in advanced aerospace, hydrospace, nuclear, defence and automotive structural applications. Typical smart materials being used as microsensors and microactuators are piezoelectric materials, magnetostrictive materials, electrorheological fluids and shape memory alloys. The coupled electromechanical properties of piezoelectric ceramics and their availability in the form of thin

these types of materials. The direct piezoelectric effect states that a strain applied to the material is converted to an electric charge. On the other hand, the converse piezoelectric effect states that an electric potential applied to the material is converted to strain. In this work, a piezolaminated beam finite element has been formulated and active vibration control performance of a beam with distributed piezoelectric sensors and actuators has been studied using different types of control strategies.

Distributed vibration control of beams using the piezoelectric effect has been studied by Bailey<sup>1</sup>, *et al.*, Crawley and Luis<sup>2</sup> and Tzou<sup>3</sup>. In terms of achieving very high damping, only limited success has been achieved by these distributed control approaches. Baz and Poh<sup>4,5</sup> have used modified independent modal space control method to study the performance of an active control system in beams with piezoelectric actuators. Crawley and Luis proposed an analytical model of the static interaction between a beam and segmented piezoelectric actuators, which were symmetrically bonded to the top and bottom surfaces of the beam. Devasia<sup>6</sup>, *et al.* have formulated actuator placement and sizing methodologies for vibration suppression in uniform beams. Several closed-loop performance criteria were considered to derive objective functions for optimum placement and sizing of piezoelectric actuators in uniform beams. Tzou<sup>7</sup> has studied the boundary control of beams. Two control algorithms, namely displacement feedback and velocity feedback were implemented and their control effectiveness evaluated. It has been shown that velocity feedback controls were much more effective. A 1-D mathematical model for determining the mechanical responses of beams with piezoelectric actuators has been proposed by Shen. This model is based on Timoshenko beam theory with the host beam and piezoelectric patches being separately modelled using beam elements. Kinematic assumptions were made to satisfy the compatibility requirements in the vicinity of the

A piezoelectric laminated elastic beam in Fig. 1 has been considered. Two thin piezoelectric material are bonded on the bottom surfaces of the beam. One layer is distributed sensor and the other as a distributed actuator. In this case, the piezoelectric material has been assumed to be monoaxially oriented (the piezoelectric constant  $d_{31} \neq 0$  and  $d_{32} = 0$ ). The effective piezoelectric layer is aligned with the direction of the beam to ensure the maximum piezoelectric effect. The signal from the distributed sensor is used as a feedback reference in a closed-loop feedback control system. The laws determined the feedback signal to be applied to the distributed actuator. In Fig. 1,  $F(t)$  is a disturbing force,  $\phi_s$  is the voltage generated by the sensor and  $\phi_a$  is the voltage given to the actuator to control the structural deformations. The signal,  $\phi_s$ , is a function of strains in the sensor. The voltage  $\phi_a$ , applied to the actuator, creates effective control forces and moments.

### 3. MODELLING & FORMULATION

The layout of a beam with distributed sensor and actuator is shown in Fig. 1. It is assumed that the piezoelectric layers are perfectly bonded to the top and bottom surface of the beam and also the bonding layer is thin. Hence, the contribution of the bonding layer on the mass and stiffness of the beam is neglected. However, the contribution of the piezoelectric sensor and actuator layers on the mass and stiffness of the beam is considered. Linear theories of piezoelectricity and perfect continuity without any slip is assumed at the interfaces. The applied voltage is assumed to be uniform along the beam.

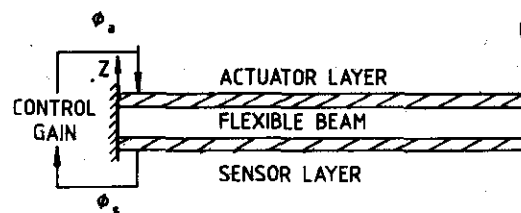


Figure 1. A cantilever beam with distributed actuator and sensor.

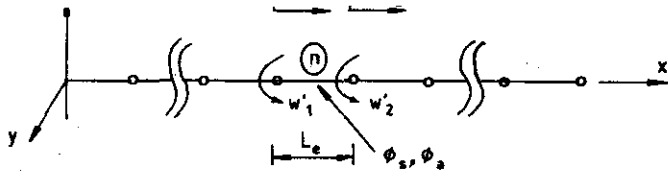


Figure 2. Finite element discretisation of beam

### 3.1 Finite Element Formulation

The geometry indicating the nodal deformations of the beam is shown in Fig. 2 represents the coordinate in the axial direction. The transverse displacement ( $w$ ) is interpolated using cubic polynomial in  $x$  defined over the element length ( $L_e$ ). The axial displacement ( $u$ ) is interpolated using linear polynomial in  $x$  defined over the  $L_e$ . The local nodal displacements for a typical element (Fig. 2) are given by

$$\{\delta\}_e = [u_1 \quad w_1 \quad w'_1 \quad u_2 \quad w_2 \quad w'_2]^T \quad (1)$$

where  $w'$  indicates the transverse rotation (slope). The axial and transverse displacements have been expressed in terms of the nodal displacements by finite element shape functions as

$$u = [N_u(x)]\{\delta\}_e; \quad w = [N_w(x)]\{\delta\}_e \quad (2)$$

where  $[N_u(x)]$  and  $[N_w(x)]$  are appropriate shape functions.

Let  $\hat{EI}$  be the effective flexural rigidity, given by the summation of the flexural rigidities of the beam, sensor and actuator layers and  $\hat{\rho A}$  the effective mass per unit length. The element stiffness and mass matrices of the beam with the piezoelectric layers are evaluated from the potential and kinetic energies due to the beam deformations and the element force vector due to external disturbance forces is evaluated from the virtual work, in the usual way. For 1-D structures with uniaxial loading, the constitutive equation of the piezoelectric materials coupling elastic and electric fields (IEEE Standard on Piezoelectricity, 1987) can be written as

where  $D$  is the electrical displacement [charge/area in the beam transverse direction ( $z$ -direction)],  $\bar{E}$  is the electrical field (voltage/length along the  $z$  direction),  $\varepsilon$  is the mechanical strain in the axial direction ( $x$ -direction), and  $\sigma$  is the mechanical stress in  $x$ -direction.  $S_{p11}$  is the elastic compliance constant,  $\varepsilon_{33}^T$  is the dielectric constant, and  $d_{31}$  is the piezoelectric strain constant.

$$S_{p11} = \frac{1}{E_p} \quad \text{and} \quad \bar{E} = \frac{\phi_p(t)}{h_p} \quad (4)$$

where  $E_p$  is the Young's modulus of the piezoelectric material,  $\phi_p$  is the voltage applied (in the case of actuator)/induced (in the case of sensor) in the piezoelectric material and  $h_p$  is the thickness of the piezoelectric material. [The subscript  $p$  represents the actuator or sensor piezoelectric layer].

The virtual work done by the induced strain (force) in the actuator is given by

$$\begin{aligned} \Delta W_a &= \int_0^{L_e} E_a d_{31a} b \phi_a(t) \Delta \left( \frac{\partial u}{\partial x} - r_a \frac{\partial^2 w}{\partial x^2} \right) dx \\ &= E_a d_{31a} b \phi_a(t) \left\{ \Delta u - r_a \Delta \left( \frac{\partial w}{\partial x} \right) \right\} \Bigg|_{x=0}^{x=L_e} \\ &= E_a d_{31a} b \phi_a(t) \{\Delta \delta\}_e^T \left[ \begin{array}{c} [N_u(L_e)] \\ [N'_w(L_e)] \end{array} \right]^T \begin{Bmatrix} 1 \\ -r_a \end{Bmatrix} \\ &\quad - \begin{Bmatrix} [N_u(0)] \\ [N'_w(0)] \end{Bmatrix}^T \begin{Bmatrix} 1 \\ -r_a \end{Bmatrix} \\ &= \{\Delta \delta\}_e^T E_a d_{31a} b \phi_a(t) \times \{-1 \quad 0 \quad r_a \quad 1 \quad 0 \quad -r_a\}^T \\ &= \{\Delta \delta\}_e^T \{P_a\}_e \phi_a(t) \end{aligned} \quad (5)$$

where  $\{P_a\}_e$  is the piezoelectric element force vector which maps the applied actuator voltage to the induced displacements and  $r_a$  is the distance measured from the neutral axis of the beam to the mid-plane of the actuator layer. (The subscript  $a$

$$\begin{aligned} \{P_a\}_e &= E_a d_{31} b \times \{-1 \ 0 \ r_a \ 1 \ 0 \ -r_a\}^T \\ &= \{-F_a \ 0 \ M_a \ F_a \ 0 \ -M_a\}^T \end{aligned} \quad (6)$$

where  $F_a$  and  $M_a$  are the axial control forces and the bending control moments, respectively. It can be noted that the piezoelectric-induced force and moment results in boundary actions at the ends of the piezoelectric layer due to the force cancellation at common nodes when continuity between elements is enforced.

Using Hamilton's principle, the equations of motion for an element can be obtained as

$$[M]_e \{\ddot{\delta}\}_e + [K]_e \{\delta\}_e = \{f_d\}_e + \{P_a\}_e \phi_a(t) \quad (7)$$

where,  $[M]_e$  is the element mass matrix and  $[K]_e$  is the element stiffness matrix obtained from the kinetic and potential energies of the beam with the piezoelectric sensor and actuator layers due to axial and bending deformations. The global equation of motion obtained by assembling the elemental equations is given by

$$[M]\{\ddot{\delta}\} + [C]\{\dot{\delta}\} = [K]\{\delta\} = \{f_d\} + \{P_a\}\phi_a(t) \quad (8)$$

where  $[C]$  is the structural damping included via Raleigh damping.

Assuming that the system response is governed by the first  $m$  modes of the system, the displacement  $\{\delta(t)\}$  can be approximated by

$$\{\delta\} \approx \sum_{j=1}^m \{\varphi\}_j \eta_j = [\hat{\Psi}]\{\eta\} \quad (9)$$

where  $\{\eta(t)\}$  are the modal coordinates,  $\{\varphi\}_j$  is the modal vector of the  $j^{\text{th}}$  mode and  $[\hat{\Psi}]$  is the truncated modal matrix with  $m$  retained modes. Using the above approximation, the equation of motion [Eqn (8)] can be transformed to the reduced modal space form as

$$[\bar{M}]\{\ddot{\eta}\} + [\bar{C}]\{\dot{\eta}\} + [\bar{K}]\{\eta\} = \{\bar{P}_a\}\{\phi_a(t)\} + \{\bar{f}_d\} \quad (10)$$

To apply the optimal control schemes like linear quadratic regulator (LQR), it is convenient to have the equations representing the dynamics of the system in a state space form. Introducing the state space variable  $\{\xi\}$  as  $\{\xi\} = \begin{Bmatrix} \dot{\eta} \\ \eta \end{Bmatrix}$ , the system

dynamics can be written in state space form as

$$\{\dot{\xi}\} = [A]\{\xi\} + [B]\{\phi_a\} + [\hat{B}]\{u_d\} \quad (11)$$

where  $[A]$  is the system matrix,  $[B]$  is the control matrix, and  $[\hat{B}]$  is the disturbance matrix. These matrices are given by

$$\begin{aligned} [A] &= \begin{bmatrix} -[\bar{M}]^{-1}[\bar{C}] & -[\bar{M}]^{-1}[\bar{K}] \\ [I] & [0] \end{bmatrix}; [B] = \begin{bmatrix} [\bar{M}]^{-1}\{\bar{P}_a\} \\ [0] \end{bmatrix}; \\ [\hat{B}] &= \begin{bmatrix} [\bar{M}]^{-1}\{\bar{f}_d\} \\ [0] \end{bmatrix} \end{aligned} \quad (12)$$

$\{u_d\}$  is the disturbance input vector and  $\{\phi_a\}$  is the control input (to actuator). The output equation can be written in the physical coordinates as

$$\{y\} = [C_o]\{\delta\} \quad (13)$$

where  $[C_o]$  is the output matrix. On transforming to modal coordinates and then to state space coordinates, Eqn (13) becomes:

$$\begin{aligned} \{\bar{y}\} &= [C_o][\hat{\Psi}]\{\eta\} = [[0] [C_o] [\hat{\Psi}]]\{\xi\} \\ &= [\bar{C}_o]\{\xi\} \end{aligned} \quad (14)$$

The state space model of the system dynamics is thus represented by Eqns (11) and (14).

### 3.2 Sensor Equations

If the sensor is extending on the beam from  $x = x_1$  to  $x = x_2$  and  $x_2 > x_1$ , (Fig. 3) then the sensor voltage ( $\phi_s$ ) contributed by the bending effect can be estimated by the normal strains in the axial

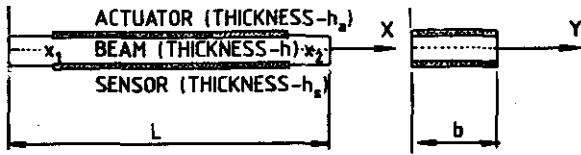


Figure 3. Layout of beam with partially covered distributed piezoelectric actuator and sensor.

direction of the beam. Thus, the sensor voltage is given by

$$\begin{aligned}\phi_s &= -\frac{h_s}{x_2 - x_1} \int_{x_1}^{x_2} g_{31} E_s r_s w_{,xx} dx \\ &= -\frac{h_s}{x_2 - x_1} g_{31} E_s r_s w_{,x} \Big|_{x_1}^{x_2}\end{aligned}\quad (15)$$

where  $h_s$  is sensor thickness,  $g_{31}$  is the piezoelectric stress constant,  $r_s$  is the distance measured from the neutral axis of the beam to the mid-plane of the sensor layer and  $E_s$  is the Young's modulus of the sensor. It can be noted from the sensor equation that the output signal is proportional to the rotation of the beam at both ends of the sensor layer. For a fully distributed sensor, that is,  $x_1 = 0$  and  $x_2 = L$ , where  $L$  is the length of the beam, the sensor voltage becomes:

$$\phi_s = -\frac{h_s}{L} g_{31} E_s r_s w_{,x} \Big|_0^L \quad (16)$$

Note that the sensor voltage is zero if the slopes at both ends of the sensor become equal, for example, antisymmetrical modes of a simply supported beam laminated with a symmetrically distributed sensor layer. In such circumstances, segmented sensors and actuators with multiinput-multioutput (MIMO) controllers can be used. After obtaining the sensor voltage  $\phi_s$ , the actuator voltage  $\phi_a$  to be applied across the actuator can be determined using any one of the control laws.

control laws based on output feedback and one optimal control law based on full-state feedback are considered. The classical control laws considered are direct proportional feedback, constant-gain negative velocity feedback and Lyapunov feedback. The optimal control law considered is LQR scheme. In classical control laws, the gains are arbitrarily chosen, whereas in the optimal control law, an optimal control gain is obtained, which minimises an objective function.

### 3.3.1 Direct Proportional Feedback Control

The direct proportional feedback control is a displacement feedback control in which the actuator voltage is generated by amplifying the sensor output directly. The control law can be expressed as

$$\phi_a(t) = G_c \phi_s(t) \quad (17)$$

where  $G_c$  denotes the voltage amplification ratio – a feedback control gain—which can be adjusted depending on the performance requirements of the system. Since the sensor signal is a function of strains, that is, displacements in the structure, this control scheme usually controls the system's natural frequencies. The amplitude can also change due to the frequency change.

### 3.3.2 Constant-Gain Negative Velocity Feedback Control

In this method of control, the sensor voltage  $\phi_s$  is differentiated so that a strain rate (related to the velocity) information is obtained and the actuator voltage ( $\phi_a$ ) is given by

$$\phi_a(t) = -G_c \dot{\phi}_s(t) \quad (18)$$

The velocity feedback can enhance the system damping and therefore effectively control the oscillation amplitude. But as the velocity amplitude decays, the feedback voltage also decreases. This will reduce the effectiveness at low vibration levels for a given voltage limit.

the velocity. The amplitude of feedback signal can be expressed as

$$\phi_a(t) = -\phi_{\max} \operatorname{sgn}[\dot{\phi}_s(t)] \quad (19)$$

where  $\operatorname{sgn}[\cdot]$  is a signum function and  $\phi_{\max}$  is the magnitude of the control voltage. This is also called bang-bang control. Note that the Lyapunov control scheme can introduce unstable oscillations due to sudden change of feedback voltage and hence a dead zone is setup, as in the following equation to prevent excessive chattering

$$\phi_a(t) = 0 \quad \text{when} \quad -\phi_{\text{dead}} < \dot{\phi}_s < \phi_{\text{dead}} \quad (20)$$

### 3.3.4 Linear Quadratic Regulator Optimal Control

LQR optimal control theory<sup>8-10</sup> is used to determine the control gains. In this, the feedback control system is designed to minimise a cost function or a performance index which is proportional to the required measure of the system's response. A state feedback rather than output feedback is adopted to enhance the control performance. The cost function used in this case is given by

$$J = \int_0^{\infty} (\bar{y})^T [Q] \bar{y} + \{\phi_a\}^T [R] \{\phi_a\} dt \quad (21)$$

where,  $[Q]$  and  $[R]$  are the semi-positive-definite and positive-definite weighting matrices on the outputs and control inputs, respectively. In this case, larger (relatively) elements in  $[Q]$  mean that more vibration suppression ability was demanded from the controller. The purpose of the second term in Eqn (21) is to account for the effort being expended by the control system, so that small reductions in the output response are not obtained at the expense of physically unreasonable actuator input levels. Assuming full-state feedback, the control law is given by

$$\{\phi_a\} = -[G_c] \{\xi\} \quad (22)$$

and  $[P]$  satisfies the Riccati equation

$$[A]^T [P] + [P] [A] - [P] [B] [R]^{-1} [B]^T [P] + [C_o]^T [Q] [C_o] = 0 \quad (24)$$

The closed-loop system dynamics is given by

$$\begin{aligned} \dot{\xi} &= ([A] - [B][G_c]) \xi + [\hat{B}] \{u_d\} \\ &= [A_{cl}] \xi + [\hat{B}] \{u_d\} \end{aligned} \quad (25)$$

where  $[A_{cl}]$  is the closed-loop system matrix. The eigenvalues of  $[A_{cl}]$  gives the damped natural frequencies and damping ratios.

It can be noted that only few states of the system could be measured as the output of the sensor, while all states of the system were used in obtaining the actuator voltage. Hence, a state observer or estimator is to be designed which could estimate all the state values from the measured signal. One such observer is the Kalman filter which is an optimal state observer for a system contaminated with process and measurement noise. An optimal control procedure that uses a Kalman filter as an observer and a controller that minimises a cost function of quadratic form is called linear quadratic gain (LQG) control method<sup>8-10</sup>. The MATLAB software has in-built functions for estimating the control gains using LQR and LQG methods. In the present work, MATLAB software has been used for solving the associated Riccati equation and obtaining the control gains in LQR control methods.

### 3.4 Actuator Equations

For a distributed piezoelectric actuator, as discussed in Eqns (5) and (6), the distributed axial control forces ( $F_a$ ) and bending control moments ( $M_a$ ) acting on the beam are given by

$$F_a = E_a d_{31_a} b \phi_a; \quad M_a = r_a E_a d_{31_a} b \phi_a \quad (26)$$

It can be noted that the control forces and moments are spatially distributed when the actuator

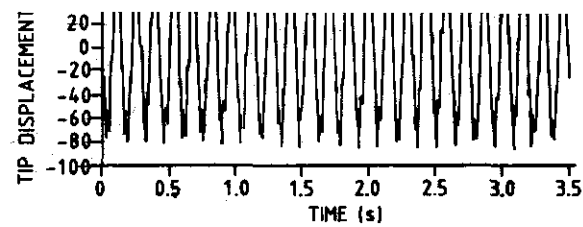


Figure 6. Tip displacement of piezolaminated cantilever beam subjected to 0.2 N impact load at the tip and controlled using direct proportional feedback (gain = 1).

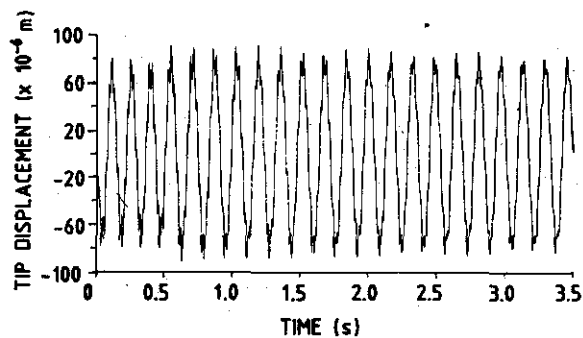


Figure 7. Tip displacement of piezolaminated cantilever beam subjected to 0.2 N impact load at the tip and controlled using direct proportional feedback (gain = 50).

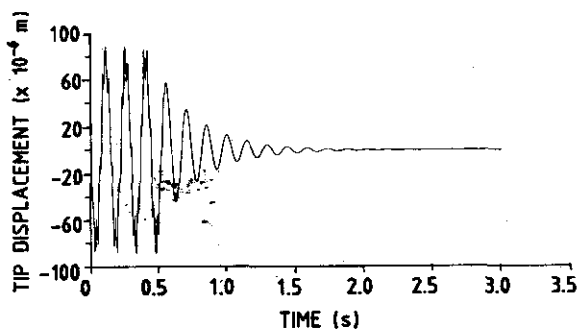


Figure 8(a). Tip displacement of piezolaminated cantilever beam subjected to 0.2 N impact load at the tip and controlled using constant-gain negative velocity feedback (gain = 1).

properties<sup>4</sup> of PZT are presented in Table 1. The beam is divided into 10 elements. The stiffness and the mass of the piezoelectric layers are included in the model. The structural damping is neglected, and the aim is to access the effectiveness of the active control. The first six natural frequencies of the

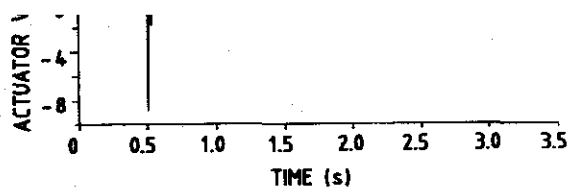


Figure 8(b). Actuator voltage corresponding to figure 8(a)

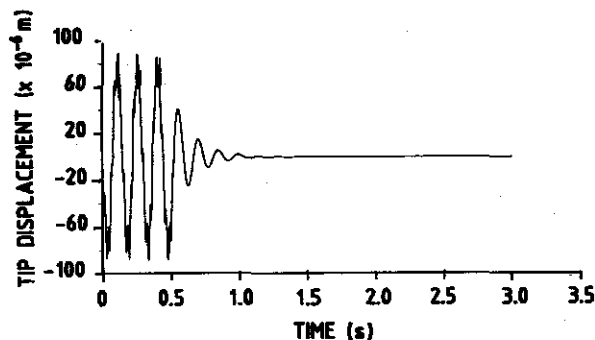


Figure 9(a). Tip displacement of piezolaminated cantilever beam subjected to 0.2 N impact load at the tip and controlled using constant-gain negative velocity feedback (gain = 2).

beam were 6.890 Hz, 43.285 Hz, 121.225 Hz, 237.720 Hz, 393.580 Hz and 589.630 Hz.

An external impulse load of 0.2 N is assumed to act at the free end of the beam for one millisecond. The control is applied after 0.5 s of the application of the load so as to have a comparison between the controlled and uncontrolled response. Figures 6 and 7 indicate the vibration control performance using direct proportional feedback with gain 1 and 50, respectively. The control performance with constant-gain negative velocity feedback with gain 1 and 2 are shown in Figs 8 and 9, respectively. It can be noted from Figs 6 and 7 that the direct proportional feedback (displacement feedback) controls are insignificant even for higher gain values. It is evident from Figs 8 and 9, that the velocity feedback controls are much more effective than the displacement feedback controls. It is because the former changes the system damping, whereas the latter changes the system's natural frequency.

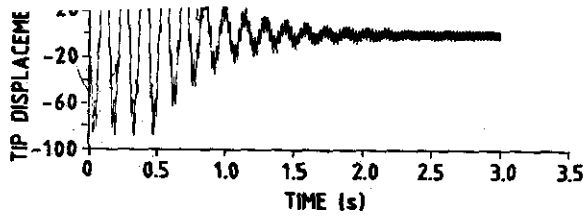


Figure 14(a). Tip displacement of piezolaminated cantilever beam subjected to 0.2 N impact load at the tip and controlled using LQR control ( $Q = 10^8$  and  $R = 1$ ).

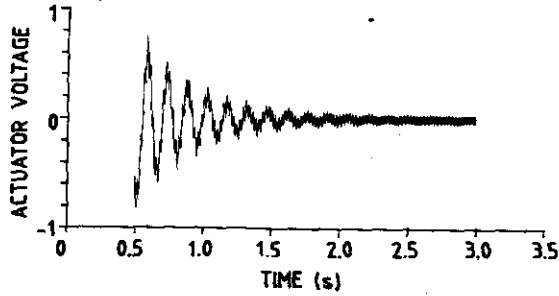


Figure 14(b). Actuator voltage corresponding to figure 14(a)

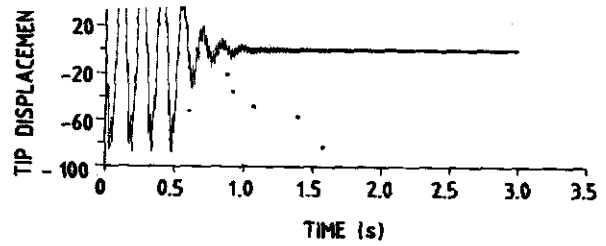


Figure 15(a). Tip displacement of piezolaminated cantilever beam subjected to 0.2 N impact load at the tip and controlled using LQR control ( $Q = 10^9$  and  $R = 1$ ).

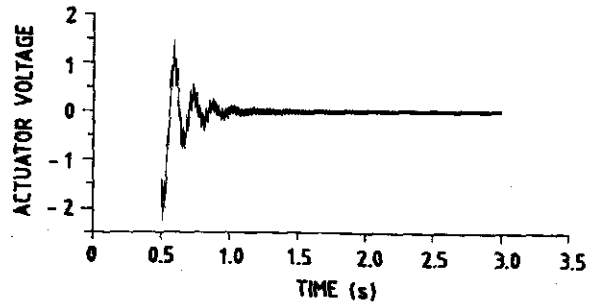


Figure 15(b). Actuator voltage corresponding to figure 15(a)

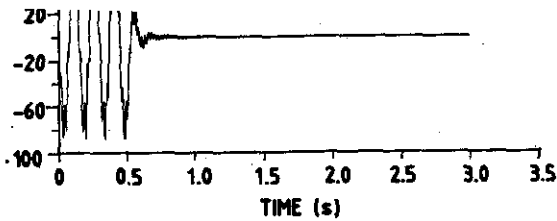
Figures 14, 15 and 16 indicate the control effectiveness using LQR optimal control with

Table 3. Damping ratio and peak actuator voltages for constant-gain negative velocity feedback and LQR control with different values of control parameters

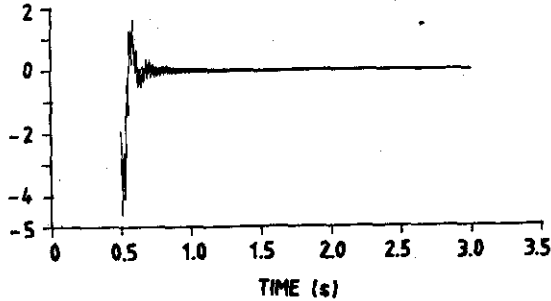
Type of control strategy	First mode damping ratios	Peak actuator voltages
Constant-gain negative velocity feedback control ( $\gamma = 0.5$ )	0.0391	14.3440
Constant-gain negative velocity feedback control ( $\gamma = 1.0$ )	0.0781	28.6880
Constant-gain negative velocity feedback control ( $\gamma = 2.0$ )	0.1560	57.3760
Constant-gain negative velocity feedback control ( $\gamma = 3.0$ )	0.2330	86.0640
LQR control ( $Q = 10^8, R = 1$ )	0.0589	0.9480
LQR control ( $Q = 10^8, R = 2$ )	0.0421	0.6696
LQR control ( $Q = 10^9, R = 1$ )	0.1742	3.0000
LQR control ( $Q = 10^{10}, R = 1$ )	0.3815	8.9800

weighting factor  $Q$  to be  $10^8$ ,  $10^9$  and  $10^{10}$ , respectively. The first mode damping factors in these cases are 0.0589, 0.1742 and 0.3815, respectively. The damping ratios and the peak actuator voltages for constant-gain negative velocity feedback and LQR control are shown in Table 3. It can be noted that LQR optimal control offered an effective control with lesser peak actuator voltages. In the present case, the gain of the constant-gain negative velocity feedback should be  $< 2$ , due to the limitation of the maximum allowable voltage of the PZT used (that is,  $1V/\mu m$ ).

The effectiveness of the active control strategy in controlling the response of the beam subjected to harmonic load is demonstrated in Figs 17 and 18 wherein harmonic loads of  $0.2 \sin(250 t)$  N and  $0.2 \sin(43.3 t)$  N are applied respectively at the free end. It can be noted that in the case indicated by Fig. 18, the harmonic load applied is near the first natural frequency.



16(a). Tip displacement of piezolaminated cantilever beam subjected to 0.2 N impact load at the tip and controlled using LQR control ( $Q = 10^{10}$  and  $R = 1$ ).



re 16(b). Actuator voltage corresponding to figure 16(a)

## SUMMARY & CONCLUSIONS

In this work, the active vibration control of  $\alpha$  like structures with distributed piezoelectric or and actuator layers bonded to top and bottom faces of the beam has been studied. A laminated beam finite element has been developed and the model is validated. The active vibration control performance has been studied using classical control laws, like direct proportional feedback, constant-gain negative velocity feedback, Lyapunov feedback and also using optimal control law based on LQR theory.

From the results it can be noted that the control effectiveness offered by direct proportional feedback, which is a displacement feedback, is significant when compared to the constant-gain negative velocity feedback and Lyapunov feedback which are velocity feedbacks. Velocity feedbacks are more effective than displacement feedbacks which is due to the fact that the former changes the system damping while the latter changes the system natural frequencies.

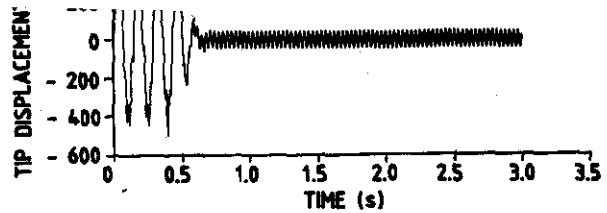


Figure 17. Tip displacement of piezolaminated cantilever beam subjected to harmonic load of  $0.2 \sin(250 t)$  N at the tip and controlled using constant-gain negative velocity feedback (gain = 1).

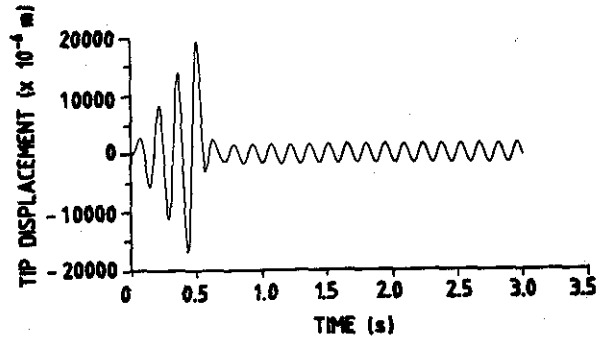


Figure 18. Tip displacement of piezolaminated cantilever beam subjected to harmonic load of  $0.2 \sin(43.3 t)$  N at the tip and controlled using constant-gain negative velocity feedback (gain = 1).

In the case of constant-gain negative velocity feedback, the damping ratio increased and reached a maximum value and then decreased, which was due to high boundary feedback voltage. Also care should be exercised such that the peak actuator voltage does not exceed the breakdown voltage of the piezoelectric layer at which the actuator loses its piezoelectric property. It can be noted from the results that Lyapunov feedback are more effective in controlling the vibration and simpler to apply, but it may introduce unstable oscillations due to sudden changes of feedback voltages, especially at high feedback voltages, and hence a dead zone is set up as in Eqn. (20), wherein the actuator voltage is maintained at zero.

The study also revealed that the LQR optimal control offers an effective control with lesser peak actuator voltages when compared to classical

using distributed sensors/actuators is effective in controlling the oscillations due to impact and harmonic loading.

## REFERENCES

1. Bailey, T. & Hubbard, J.E. Distributed piezoelectric-polymer active vibration control of a cantilever beam. *J. Guid. Control*, 1985, 8, (5), 605-11.
2. Crawley, E.F. & Luis, J. De. Use of piezoelectric actuators as elements of intelligent structures. *AIAA Journal*, 1987, 25 (10), 1373-385.
3. Tzou, H.S. Integrated distributed sensing and active vibration suppression of flexible manipulators using distributed piezoelectrics. *J. Robot. Syst.*, 1989, 6 (6), 745-67.
4. Baz, A; & Poh, S. Performance of an active control system with piezoelectric actuators. *J. Sound Vib.*, 1988, 126 (2), 327-43.
5. Tzou, H.S. *Active Vibration Control*, 1994, 114, 96-103.
6. Devasia, S.M.; Meressi, T.; Panden, B. & Bayo, E. Piezoelectric actuator design for vibration suppression—placement and sizing. *J. Guid. Control Dyn.*, 1993, 16 (5), 859-64.
7. Tzou, H.S. Piezoelectric shells—distributed sensing and control of continua, Kluwer Academic, London. 1993.
8. Kwakernaak, H. & Sivan, R. *Linear optimal control systems*. John Wiley & Sons, Inc., New York, 1972.
9. Ogata, K. Designing linear control systems with Matlab. Prentice Hall, Englewood Cliffs, New Jersey, 1994.
10. Fuller, C.R.; Elliott, S.J. & Nelson, P.A. Active control of vibration. Academic Press Ltd., London, 1996.

## Contributors



**Shri V Balamurugan** did his BE from the Anna University in 1991 and MS from Indian Institute of Technology (IIT) Madras, in 2000. Currently, he is pursuing his research for PhD in the Dept. of Applied Mechanics, IIT Madras. Presently, he is working as Scientist at the Combat Vehicles Research & Development Establishment (CVRDE), Chennai. His areas of interest include: structural dynamics and stress analysis using finite element method, active vibration control, smart structures, etc.



**Dr S Narayanan** obtained his PhD from IIT, Kanpur and is presently working as Professor in the Dept. of Applied Mechanics, IIT Madras. He is also Dean (Academic Research) at IIT. He is a fellow of Indian National Academy of Engineering, President of Acoustical Society of India. His areas of interest include: Random vibrations, nonlinear dynamics, chaos, dynamics of machinery, vehicle dynamics, active suspension, active vibration and noise control with smart structures, etc.